Study on Stress-Temperature Coupled Damage Model of Warm Frozen Soil

Wei Shan, Tao Yang , Ying Guo, Chengcheng Zhang

Cold region science and engineering institute, Northeast Forestry University, China.

Corresponding author: Wei Shan (shanwei456@163.com)

Key Points:

- The model can effectively predict the stress-strain relationship of warm frozen soil under the coupling effect of stress and temperature.
- When strain softening, the shape and scale parameters are better solved according to the characteristic points of stress-strain curve.
- Compared with the single stress damage model, the model can effectively reduce the influence of parameter estimation error on the results.

Abstract

Warm frozen soil is very sensitive to temperature change in the near phase transition region, and the relationship between temperature and physical and mechanical properties can be expressed by constitutive model. Based on the strain equivalent theory of damage mechanics, the damage model of warm frozen soil structure under the coupling action of stress and temperature is established. Based on Mohr- Coulomb criterion, the nominal stress is used to represent the stress damage of frozen soil element, the initial elastic modulus is used to represent the temperature damage, and the composite damage factor is introduced to describe the coupling relationship between them. Two methods are used to obtain the shape parameters and scale parameters of the coupled damage model: method 1 is the full fitting method based on the experimental data; method 2 is the semi theoretical semi fitting method based on the characteristic points of the stress-strain curve. Through the triaxial compression test of frozen sand, it is proved that the simulation results of the stress-temperature coupled damage model are in good agreement with the experimental curves. Based on the experimental results, the results of the two methods are compared, and it is proved that method 2 is better than method 1 under the condition of strain softening. By comparing the predicted results of stress temperature coupled damage model and single stress damage model, it is shown that the former can effectively reduce the influence of parameter estimation error on the results and improve the stability of the model.

1 Introduction

With the global warming and the rise of ground temperature, permafrost gradually degenerates and the warm frozen soil stock further increases(Wei et al., 2011; Zhou et al., 2000) .There is a close dynamic equilibrium relationship between the unfrozen water content and the temperature. As a cemented phase, ice has a crucial influence on the mechanical properties of frozen soil. The unfrozen water is very sensitive to the change of temperature in the near phase transition region of warm frozen soil. Small temperature difference will directly lead to the change of unfrozen water membrane thickness of frozen soil particles. The difference is reflected in the mechanical index of frozen soil element and will be enlarged to a certain extent(Jin et al., 2019; Xu, XZ et al., 2001; Yan et al., 2019). Compared with normal frozen soil, warm frozen soil is essentially similar to the mixed state of thawed soil and frozen soil(Liu, S&Zhang, 2012). This kind of material form makes the internal defects of permafrost unit more significant than that of normal permafrost in terms of both the relative quantity and the influence on the mechanical properties of soil(Lai et al., 2008; Li, S et al., 2009; Ning&Zhu, 2007). Due to the high instantaneous strength of frozen soil, the elastic modulus of frozen soil is assumed to be a certain value in numerical calculation(Liu, Z&Yu, 2011; Na&Sun, 2017; Zhang, M et al., 2017; Zhang, Y&Michalowski, 2015). But for warm frozen soil, because of the increase of unfrozen water content caused by the increase of temperature, the deterioration of frozen soil stiffness will be more obvious(Jia et al., 2019). In the variable temperature environment, if the mechanical parameters under a certain temperature fixed value are used for the numerical analysis of the stress-strain relationship of frozen soil, it is easy to have problems such as the calculation result error is too large, which will affect the safety of the facilities(Li, G, 2009).

The mechanical research of warm frozen soil mainly focuses on its strength characteristics, deformation characteristics and constitutive model, but the overall research of constitutive model is less(Liu, S&Zhang, 2012). Lai Yuanming et al. (Lai et al., 2008; Li, S et al., 2007)Showed that the distribution of strength and elastic modulus of warm frozen soil is discrete. The distribution of strength and elastic modulus of frozen soil can be described by Weibull distribution. Strain is taken as damage token and statistical damage mechanics is introduced to form the earliest damage model of warm frozen soil. According to Li Shuangyang et al. (Li, S et al., 2009), the concept of mechanical damage represented by strain is not clear enough and lacks theoretical support. Therefore, Mohr-Coulomb criterion is introduced to judge the damage state of warm frozen soil element, and the parameter expression in one-dimensional state is derived, which has achieved good results. The constitutive study of warm frozen soil has always focused on the deformation development under the action of single stress factor, and temperature is only a fixed condition rather than an action factor, which limits the application scope of the constitutive model to a certain extent(Lai et al., 2009; Zhang, D et al., 2018). At present, the research on the coupling effect of stress and temperature is mainly focused on the level of physical field control equation, while the research on the deeper constitutive model is less (Dumais & Konrad, 2017; Zhang, Y&Michalowski, 2015). According to the strain equivalent theory of damage mechanics, Zhang Huimei et al. (Zhang, H&Yang, 2010) obtained the composite damage model of freeze-thaw rock under the action of temperature and stress. Yu Songtaoet al.(Yu et al., 2018)introduced H-B criterion to extend the application scope of the model to describe the stress-strain relationship of rock under the action of warm and confining pressure.

In view of the above problems and shortcomings, this paper introduces the composite damage theory into the stress-strain simulation prediction of warm frozen soil, establishes the stress-temperature coupling damage model characterized by Mohr-Coulomb criterion for the three-dimensional stress damage state of warm frozen soil element, and verifies the prediction effect of the model through relevant experiments, and discusses its effectiveness and stability.

2 Stress-temperature coupled damage model

Under the combined action of stress and temperature, the internal initial state of warm frozen soil will be damaged, some of the existing damage defects will further develop, and new damage defects will gradually form (Lai et al., 2008; Li, S et al., 2009). According to the damage theory of continuous medium, with the external action, the development of this kind of damage will show the decrease of the actual stress element in the stress body, which can be understood as the damage of material structure(Lemaitre, 2012). It is reflected in the physical parameters of the material, which is the reduction of the original material parameters, described by the damage factor. Under the action of nominal stress, the nominal strain due to material degradation is as follows:

$$\varepsilon = \frac{\sigma}{\tilde{E}} = \frac{\sigma}{(1-D)\cdot E} \tag{1}$$

Where: σ is the nominal stress, ε is the nominal strain, E is the effective elastic modulus, E is the initial state of the elastic modulus.

2.1 Stress damage

Under the action of simple stress, the damage factor D_m can be expressed by the ratio of the number of damage elements $N(t)$ at a certain time to the number of damage elements N at the final failure:

$$D_m = \frac{N(t)}{N} \tag{2}$$

A large number of experiments show that $N(t)$ obeys Weibull distribution(Lai et al., 2008). Its probability density function is:

$$f(x) = \frac{m}{a} \cdot \left(\frac{x}{a}\right)^{m-1} \cdot \exp\left[-\left(\frac{x}{a}\right)^{m}\right] \tag{3}$$

Where m and a are the shape parameters and scale parameters of the distribution respectively.

So the expression of $N(t)$ is:

$$\begin{aligned} N(t) &= \int_0^F N \cdot f(x)dx \\ &= N \cdot \left\{1 - \exp\left[-\left(\frac{F}{a}\right)^{m}\right]\right\} \end{aligned} \tag{4}$$

Therefore:

$$D_m = \frac{N(t)}{N} = 1 - \exp\left[-\left(\frac{F}{a}\right)^{m}\right] \tag{5}$$

Among them, for the characterization of the number of unit damage F , Mohr-Coulomb theoretical analysis is used to determine(Li, S et al., 2009).

In triaxial compression test, Mohr-Coulomb shear strength formula can be expressed as follows by axial stress σ_1 and confining pressure σ_3 :

$$\frac{1}{2} \cdot (\sigma_1 - \sigma_3) = c \cdot \cos\varphi - \frac{1}{2} \cdot (\sigma_1 + \sigma_3) \cdot \sin\varphi \tag{6}$$

If the terms σ_1 and σ_3 in the above formula are transferred, we can get:

$$F = 2c \cdot \cos\varphi = (1 + \sin\varphi) \cdot \tilde{\sigma}_1 - (1 - \sin\varphi) \cdot \tilde{\sigma}_3 \tag{7}$$

Among them, σ_1 and σ_3 are the real stress of the material with the development of warm frozen soil damage. From the generalization of Formula 1, we can get:

$$\varepsilon = \frac{\sigma}{(1 - D_m) \cdot E} = \frac{\tilde{\sigma}}{E} \tag{8}$$

Thus, the damage characterization quantity expressed by nominal stress F can be established

$$F = \left[\left(1+\sin\varphi\right)\cdot\sigma_1 - \left(1-\sin\varphi\right)\cdot\sigma_3\right] \Big/ \left(1-D_m\right) \tag{9}$$

According to the stress-strain relationship of materials under the action of three-dimensional stress, it can be concluded that:

$$\begin{aligned}\varepsilon_1 &= \frac{1}{\tilde{E}}\cdot\left[\sigma_1 - \nu\cdot\left(\sigma_2+\sigma_3\right)\right] \\ &= \frac{1}{E\cdot(1-D_m)}\cdot\left[\sigma_1 - \nu\cdot\left(\sigma_2+\sigma_3\right)\right]\end{aligned} \tag{10}$$

In the triaxial compression experiment, $\sigma_2 = \sigma_3$, the expression of $1-D_m$ can be obtained by taking the above formula:

$$1-D_m = \left(\sigma_1 - 2\nu\cdot\sigma_3\right) \Big/ E\cdot\varepsilon_1 \tag{11}$$

Take equation (11) into equation (9) to get:

$$F = E\cdot\varepsilon_1\cdot\left[\left(1+\sin\varphi\right)\cdot\sigma_1 - (1-\sin\varphi)\cdot\sigma_3\right] / (\sigma_1 - 2\nu\cdot\sigma_3) \tag{12}$$

When the damage characterization F corresponding to different axial strain ε_1 is calculated from the above formula, σ_1 in the formula is the unknown quantity to be solved.

It is assumed that in a small strain range, the damage evolution amount of frozen soil element is small, and when reflected on the damage characterization amount F, the increment in the small range can be ignored, so it can be expressed as follows:

$$F_n = \begin{cases} E\cdot\varepsilon_{1_n}\cdot\left[\left(1+\sin\varphi\right)\cdot\sigma_{1_{n-1}} - (1-\sin\varphi)\cdot\sigma_{3_{n-1}}\right] / (\sigma_{1_{n-1}} - 2\nu\cdot\sigma_{3_{n-1}}) & n=1 \\ E\cdot\varepsilon_{1_{n-1}}\cdot\left[\left(1+\sin\varphi\right)\cdot\sigma_{1_{n-1}} - (1-\sin\varphi)\cdot\sigma_{3_{n-1}}\right] / (\sigma_{1_{n-1}} - 2\nu\cdot\sigma_{3_{n-1}}) & n\geq 2 \end{cases} \tag{13}$$

Where the lower right corner mark n represents the accumulated step number of strain ε when it is accumulated from $\varepsilon = 0$ in a certain step. When $n-1=0$, it is the stress value corresponding to the initial state before the bias load starts after the end of the confining pressure load. At this time, $\sigma_1 = \sigma_3$, the above formula can be converted into the following form:

$$F_n = \begin{cases} 2E\cdot\varepsilon_{1_n}\cdot\sin\varphi / (1-2\nu) & n=1 \\ E\cdot\varepsilon_{1_{n-1}}\cdot\left[\left(1+\sin\varphi\right)\cdot\sigma_{1_{n-1}} - (1-\sin\varphi)\cdot\sigma_{3_{n-1}}\right] / (\sigma_{1_{n-1}} - 2\nu\cdot\sigma_{3_{n-1}}) & n\geq 2 \end{cases} \tag{14}$$

2.2 Temperature damage

The cementation force of ice on soil particles and its own strength in frozen soil provide rigidity higher than that in melting state (Ning&Zhu, 2007). With the change of temperature, the strength of ice decreases and the cementation ability decreases. This kind of composite material degradation due to the effect of temperature can also be reflected by the concept of damage.

It can be seen from Formula 1 that the effect of material damage on mechanical parameters is most directly reflected in the reduction of elastic modulus.

Therefore, the temperature damage factor D_T is defined, which represents the deterioration degree of the initial state caused by the increase of temperature and the decrease of ice strength and cementation force in the frozen soil:

$$D_T = 1 - \frac{E_T}{E} \tag{15}$$

Where E is the elastic modulus of warm frozen soil in the initial state, and E_T is the elastic modulus of a certain temperature after heating up.The relationship between the elastic modulus of frozen soil and temperature can be expressed by the following formula(Zhang, M et al., 2017):

$$E_T = \beta + \gamma \cdot |T|^{0.6} \tag{16}$$

β and γ are the experimental parameters.

2.3 Coupling effect of stress and temperature

According to the theory of strain equivalence, the composite damage caused by temperature and stress can be deduced. It can be characterized by composite damage factors D_c (Zhang, H&Yang, 2010):

$$D_c = D_m + D_T - D_m \cdot D_T \tag{17}$$

Take formula (5) and formula (15) into formula (17) to get:

$$D_c = 1 - \frac{E_T}{E} \cdot \exp\left[-(\frac{F}{a})^m \right] \tag{18}$$

Take equation (16) into equation (18) and simplify it to obtain:

$$D_c = 1 - \frac{1 + \lambda \cdot |T|^{0.6}}{1 + \lambda \cdot |T_0|^{0.6}} \cdot \exp\left[-(\frac{F}{a})^m \right] \tag{19}$$

Where T_0 is the temperature of the initial state and λ is defined as the temperature deterioration coefficient:

$$\lambda = \frac{\gamma}{\beta} \tag{20}$$

Equation (19) is introduced into equation (1), which is the stress-temperature coupled damage model of worm frozen soil:

$$\varepsilon_1 = \frac{(\sigma_1 - 2\nu \cdot \sigma_3) \cdot [1 + \lambda \cdot |T_0|^{0.6}]}{[1 + \lambda \cdot |T|^{0.6}] \cdot \exp\left[-\left(\frac{F}{a} \right)^m \right] \cdot E} \tag{21}$$

3 Model parameter

The stress damage of warm frozen soil accords with the Weibull distribution(Li, S et al., 2007). The shape parameter m and scale parameter a in this distribution are two important parameters in the stress-temperature coupling model. Their values are directly affected by the stress-strain curve. Due to the different confining pressure and soil properties, the curves of deviator stress $\sigma_1-\sigma_3$ and axial strain ε_1 obtained from triaxial test of warm frozen soil will take different forms(Li, G, 2009; Song et al., 2019).

In general, the stress-strain curves of frozen sand, frozen silty sand and frozen silty clay with high moisture content will show strain softening type, and the partial stress has a peak value. After the peak strain, the partial stress decreases with the increase of strain(Esmaeili-Falak et al., 2017; Qi&MA, 2010; Xu, Xiangtian et al., 2016). For the fine-grained soil with low water content, the stress-strain curve has no obvious peak value, and the partial stress gradually increases with the increase of axial strain, but the growth rate gradually decreases, and finally tends to be stable(Ma et al., 1999).

For two different stress-strain curves, there are two typical two parameter solutions of Weibull distribution.

One is to get the values of shape parameters m and scale parameters a by linear fitting (method 1).The other is to further deduce formula (12) through the data of characteristic points in the stress-strain curve, and obtain the expression of shape parameters m and scale parameters a expressed by the numerical value of characteristic points (method 2) (Cao&Zhang, 2005; Xu, W&Wei, 2002).

Method 1: this method can be applied to both strain hardening and strain softening stress-strain curves.

Joint formula (5) and (11)

$$\exp\left[-\left(\frac{F}{a}\right)^m\right]=\left(\sigma_1-2v\cdot\sigma_3\right)/E\cdot\varepsilon_1 \tag{22}$$

The following formula can be obtained by two logarithm operations at both ends of the equation:

$$\ln\left\{-\ln\left[\left(\sigma_1-2v\cdot\sigma_3\right)/E\cdot\varepsilon_1\right]\right\}=m\ln F-m\ln a \tag{23}$$

Among them, the left-hand items and the right-hand F of the equation can be obtained through the triaxial experiment. Therefore order:

$$\mathrm{Y}=\ln\left\{-\ln\left[\left(\sigma_1-2v\cdot\sigma_3\right)/E\cdot\varepsilon_1\right]\right\} \tag{24}$$

$$X=\ln F \tag{25}$$

$$C=-m\ln a \tag{26}$$

Then we can get the linear relationship of the three:

$$Y=mX+C \tag{27}$$

A set of X and Y values corresponding to the experimental curve under a certain confining pressure and temperature can be obtained by introducing the triaxial experimental values. The expression of the final shape parameters m and scale parameters a can be obtained by linear fitting and further calculation:

$$m = \frac{Y - C}{X} \tag{28}$$

$$a = \exp(-\frac{C}{m}) \tag{29}$$

The detailed calculation method of relevant parameters will be further explained in the later experimental verification part.

Method 2: this method is only suitable for strain softening.

First, deform equation (22) to obtain:

$$\begin{aligned} \sigma_1 &= \tilde{E} \cdot \varepsilon_1 + 2v \cdot \sigma_3 \\ &= E \cdot \varepsilon_1 \cdot \exp\left[-\left(\frac{F}{a} \right)^m \right] + 2v \cdot \sigma_3 \end{aligned} \tag{30}$$

According to the generalized Hooke's law, the relationship between ε_3 and axial stress σ_1, confining pressure σ_3 can be established.

$$\begin{aligned} \varepsilon_3 &= \frac{1}{\tilde{E}} \cdot \left[\sigma_3 - v \cdot \left(\sigma_1 + \sigma_2 \right) \right] \\ &= \frac{1}{E \cdot (1 - D_m)} \cdot \left[(1 - v) \cdot \sigma_3 - v \cdot \sigma_1 \right] \end{aligned} \tag{31}$$

If the above formula is deformed and brought in (5), you can get:

$$\begin{aligned} \sigma_3 &= \left(\tilde{E} \cdot \varepsilon_3 + v \cdot \sigma_1 \right) \Big/ (1 - v) \\ &= \left(E \cdot \varepsilon_3 \cdot \exp\left[-\left(\frac{F}{a} \right)^m \right] + v \cdot \sigma_1 \right) \Big/ (1 - v) \end{aligned} \tag{32}$$

Taking the peak stress of strain softening curve as the characteristic point, the following relationship can be obtained:

$$\begin{cases} \varepsilon_1 = \varepsilon_p \\ \sigma_1 = \sigma_p \end{cases} \tag{33}$$

$$\begin{cases} \varepsilon_1 = \varepsilon_p \\ \dfrac{d\sigma_1}{d\varepsilon_1} = 0 \end{cases} \tag{34}$$

Find the total differential of formula (30) and formula (32), and the results are as follows:

$$d\sigma_1 = \frac{\partial \sigma_1}{\partial \varepsilon_1} d\varepsilon_1 + \frac{\partial \sigma_1}{\partial F} dF + \frac{\partial \sigma_1}{\partial a} da + \frac{\partial \sigma_1}{\partial m} dm + 2\nu d\sigma_3 \tag{35}$$

$$d\sigma_3 = \frac{\partial \sigma_3}{\partial \varepsilon_3} d\varepsilon_1 + \frac{\partial \sigma_3}{\partial F} dF + \frac{\partial \sigma_3}{\partial a} da + \frac{\partial \sigma_3}{\partial m} dm + \frac{\nu}{1-\nu} d\sigma_1 \tag{36}$$

The selected damage characterization quantity is determined based on Mohr-Coulomb theory. When equation (30) is brought into equation (7), the F expressed by ε_1 and σ_3 can be obtained. For the convenience of distinction, the F is marked as F^1:

$$F^1 = (1+\sin\varphi)\cdot(E\cdot\varepsilon_1 + 2\nu\cdot\sigma_3) - (1-\sin\varphi)\cdot\sigma_3 \tag{37}$$

In the same way, if you take equation (32) into equation (7), you can get F represented by ε_3 and σ_3, marked F^3:

$$F^3 = (1+\sin\varphi)\cdot(\frac{1-\nu}{\nu}\cdot\sigma_3 - \frac{E}{\nu}\cdot\varepsilon_3) - (1-\sin\varphi)\cdot\sigma_3 \tag{38}$$

Find the total differential of formula (37) and formula (38), and the results are as follows:

$$dF^1 = \frac{\partial F^1}{\partial \varepsilon_1} d\varepsilon_1 + \frac{\partial F^1}{\partial \sigma_3} d\sigma_3 \tag{39}$$

$$dF^3 = \frac{\partial F^3}{\partial \varepsilon_3} d\varepsilon_3 + \frac{\partial F^3}{\partial \sigma_3} d\sigma_3 \tag{40}$$

In the application of frozen soil damage model, the shape parameter m and the scale parameter a are often regarded as only related to the confining pressure σ_3 (Li, S et al., 2009; Zhang, D et al., 2018), so the following relationship can be obtained:

$$da = \frac{\partial a}{\partial \sigma_3} d\sigma_3 \tag{41}$$

$$dm = \frac{\partial m}{\partial \sigma_3} d\sigma_3 \tag{42}$$

If equation (39), (41) and (42) are introduced into equation (35), the total differential relations of σ_1, σ_3 and ε_1 can be obtained:

$$d\sigma_1 = (\frac{\partial \sigma_1}{\partial \varepsilon_1} + \frac{\partial \sigma_1}{\partial F}\cdot\frac{\partial F^1}{\partial \varepsilon_1}) d\varepsilon_1 + P d\sigma_3 \tag{43}$$

Upper form:

$$P = \frac{\partial \sigma_1}{\partial F}\cdot\frac{\partial F^1}{\partial \sigma_3} + \frac{\partial \sigma_1}{\partial a}\cdot\frac{\partial a}{\partial \sigma_3} + \frac{\partial \sigma_1}{\partial m}\cdot\frac{\partial m}{\partial \sigma_3} + 2\nu \tag{44}$$

If equation (40), (41) and (42) are introduced into equation (36), the total differential relations of σ_1, σ_3 and ε_3 can be obtained:

$$\frac{v}{v-1}d\sigma_1=(\frac{\partial\sigma_3}{\partial\varepsilon_3}+\frac{\partial\sigma_3}{\partial F}\cdot\frac{\partial F^2}{\partial\varepsilon_3})d\varepsilon_3+Qd\sigma_3 \tag{45}$$

Upper form:

$$Q=\frac{\partial\sigma_3}{\partial F}\cdot\frac{\partial F^2}{\partial\sigma_3}+\frac{\partial\sigma_3}{\partial a}\cdot\frac{\partial a}{\partial\sigma_3}+\frac{\partial\sigma_3}{\partial m}\cdot\frac{\partial m}{\partial\sigma_3}-1 \tag{46}$$

The total differential relations of σ_1, ε_1 and ε_3 can be obtained by combining equations (43) and (45):

$$d\sigma_1=Rd\varepsilon_1+Sd\varepsilon_3 \tag{47}$$

Upper form:

$$R=\frac{\partial\sigma_1}{\partial\varepsilon_1}=\frac{(1-v)\cdot Q}{v\cdot P+Q\cdot(1+v)}\cdot(\frac{\partial\sigma_1}{\partial\varepsilon_1}+\frac{\partial\sigma_1}{\partial F}\cdot\frac{\partial F^1}{\partial\varepsilon_1}) \tag{48}$$

$$S=\frac{\partial\sigma_1}{\partial\varepsilon_3}=\frac{(1-v)\cdot Q}{v\cdot P+Q\cdot(1+v)}\cdot(\frac{\partial\sigma_3}{\partial\varepsilon_3}+\frac{\partial\sigma_3}{\partial F}\cdot\frac{\partial F^2}{\partial\varepsilon_3}) \tag{49}$$

The numerical conditions of the characteristic points of the stress-strain curve are introduced to solve the problem. First, formula (33) is introduced into formula (30) to obtain:

$$\exp\left[-\left(\frac{F_p}{a}\right)^m\right]=\frac{\sigma_p-2v\cdot\sigma_3}{E\cdot\varepsilon_p} \tag{50}$$

Upper form:

$$F_p=(1+\sin\varphi)\cdot(E\cdot\varepsilon_p+2v\cdot\sigma_3)-(1-\sin\varphi)\cdot\sigma_3 \tag{51}$$

Then formula (34) is introduced into formula (48) and simplified to obtain:

$$\frac{\partial\sigma_1}{\partial\varepsilon_1}\Big|_{\varepsilon_1=\varepsilon_p}+\frac{\partial\sigma_1}{\partial F}\cdot\frac{\partial F^1}{\partial\varepsilon_1}\Big|_{\varepsilon_1=\varepsilon_p}=0 \tag{52}$$

After each value is brought in, it can be simplified to obtain:

$$\left(\frac{F_p}{a}\right)^m=\frac{F_p}{E\cdot\varepsilon_p\cdot(1+\sin\varphi)\cdot m} \tag{53}$$

The expression of shape parameter m and scale parameter a can be obtained by combining formula (50) and formula (53):

$$m=F_p\Big/E\cdot\varepsilon_p\cdot(1+\sin\varphi)\cdot\ln\frac{E\cdot\varepsilon_p}{\sigma_p-2v\cdot\sigma_3} \tag{54}$$

$$a=F_p\cdot\left[\frac{E\cdot\varepsilon_p\cdot(1+\sin\varphi)\cdot m}{F_p}\right]^{1/m} \tag{55}$$

The values in the above two formulas can be obtained from the curves of deviator stress and axial strain in triaxial compression experiments. If the confining pressure $\sigma_3 = 0$, formula (54) and formula (55) are reduced to one-dimensional uniaxial compression:

$$m = 1 \Big/ \ln \frac{E \cdot \varepsilon_p}{\sigma_p} \tag{56}$$

$$a = F_p \cdot (\mathrm{m})^{\frac{1}{m}} \tag{57}$$

Comparisons show that the results of uniaxial compression derived by predecessors are the same(Li, S et al., 2009).

4 Experimental verification

4.1 Determination of basic parameters

The model parameters are determined by temperature-controlled triaxial compression test of frozen sand. The composition of fine sand particles used is shown in Table 1.

Table 1. *Particle Composition of Fine Sand for Experiment*

Particle composition/%				
>0.5mm	0.5～0.25mm	0.25～0.10mm	0.10～0.075mm	<0.075mm
2.7	30.6	43.9	19.7	3.1

The specimens with diameter of 39.1mm, height of 80mm and dry weight of 15.3kN/m^3 after compaction preparation were saturated and frozen for 48h in a low temperature tank at -25℃. Three sets of triaxial compression experiments were carried out at a loading rate of 1 mm/min and a temperature of -0.3℃, -1℃, and -2℃, respectively, at a constant temperature of 24h in the target temperature chamber before the experiment. The confining pressures of each group were 50 kPa, 150 kPa and 250 kPa, respectively. The experimental results are shown in Figure. 1.

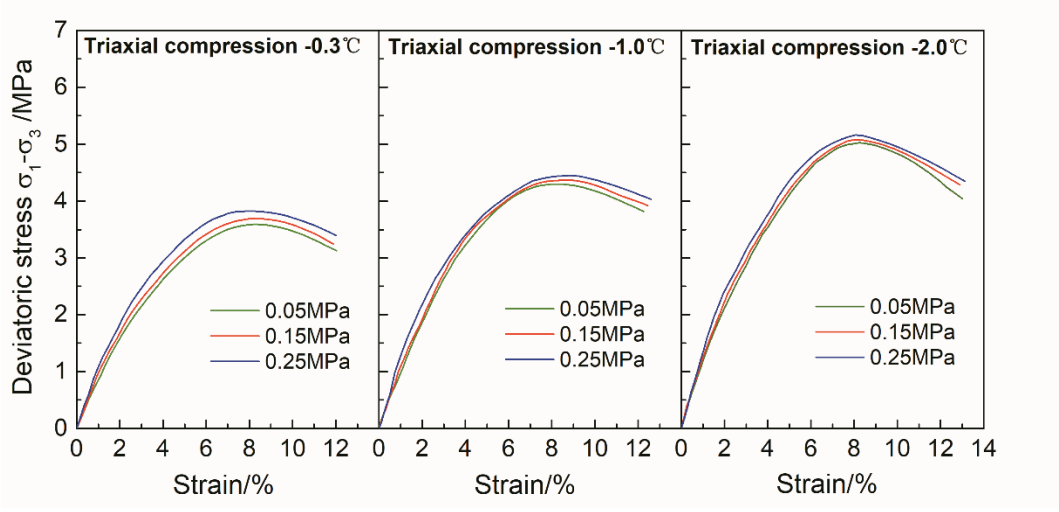

Figure 1. *Triaxial compression test stress-strain curve of frozen sand*

As can be seen from Figure. 1, the stress-strain curve approximates a linear change at the initial stage of strain. The elastic modulus of equation (15) characterizes the initial undamaged state of the frozen soil, and the closer the value is to the initial elastic modulus, the more precise the model solution is. Therefore, the modulus of the linear elastic section in the range of 0-0.5% strain is approximated as the elastic modulus E of the initial damage state.The basic mechanical parameters calculated from the experimental results are shown in Table 2.

Table 2. *Basic Mechanical Parameters of the Model*

Temperature/℃	-0.3			-1.0			-2.0		
Confining pressure/MPa	E /MPa	φ/°	ν	E /MPa	φ/°	ν	E /MPa	φ/°	ν
0.05	91.16			109.33			128.39		
0.15	97.12	21.56	0.2623	114.95	15.85	0.2513	135.85	14.66	0.2452
0.25	101.51			118.51			140.84		

According to the data in Table 2, the expression of temperature damage modulus E_T in the stress temperature coupled damage model can be obtained from equation (16).

It can be seen from the above analysis that in theory, only the confining pressure is required to be controlled, and β and γ in equation (16) should be a pair of constants. The elastic modulus values corresponding to the three groups of confining pressures in Table 2 are fitted and calculated, and the temperature damage factor D_T corresponding to the fitting curve is compared. The results are shown in Figure. 2.

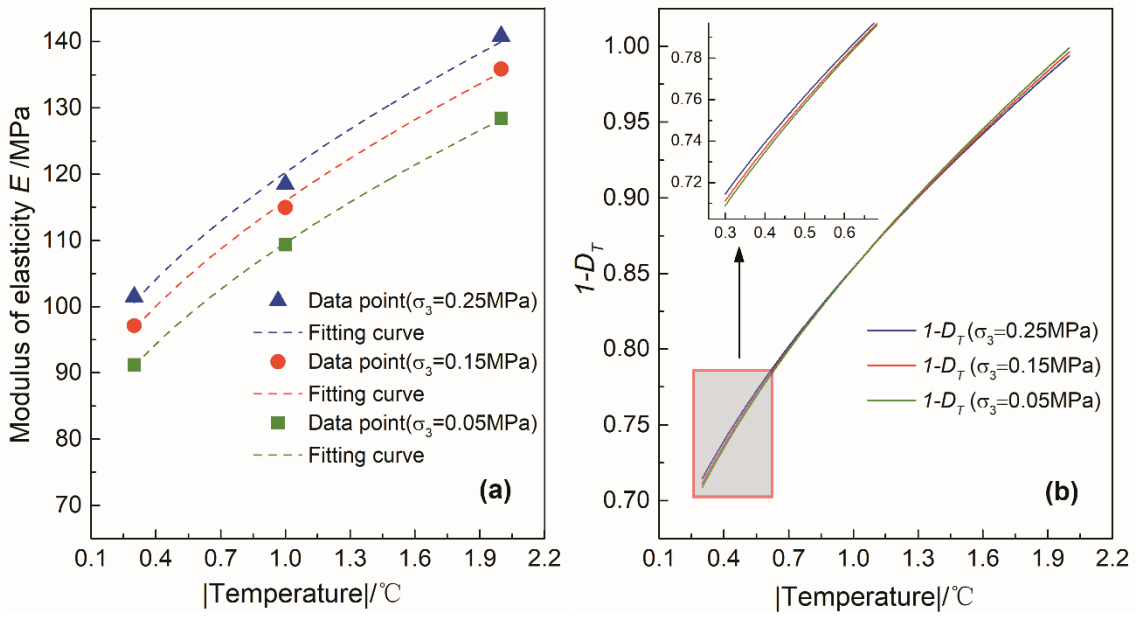

Figure2.*Fitting curve of elastic modulus and corresponding damage factors under different confining pressures.(a) Fitting curve of initial modulus of elasticity with temperature under three confining pressures 0.05MPa,0.15MPa and 0.25MPa.(b) Temperature damage factors corresponding to three confining pressure states 0.05MPa,0.15MPa and 0.25MPa when -2 ℃ is taken as non-destructive state.*

It can be seen from Figure. 2 (a) that although the fitting curves corresponding to the three groups of data are not the same, Figure. 2 (b) shows that the change curve of the final

damage factor is basically the same, so the fitting curve corresponding to the data with confining pressure of 0.05MPa is selected as the expression of elastic modulus E_T .

$$E_T = 73.47 + 36.14|T|^{0.6} \tag{58}$$

The goodness of fit $R^2 = 0.9998$, which can reflect the change of data more accurately.

It can be seen from table 2 that when the confining pressure changes, the elastic modulus will also change. In order to make the model more applicable, it is necessary to fit the relationship between elastic modulus and confining pressure at the same temperature.

In the verification experiment, the nondestructive temperature is -2.0 ℃(Liu, S&Zhang, 2012), and the relationship between elastic modulus and confining pressure is:

$$E = 123.73 + 99.3\sigma_3 - 123.5\sigma_3^{\ 2} \tag{59}$$

The fitting curve is shown in Figure. 3.

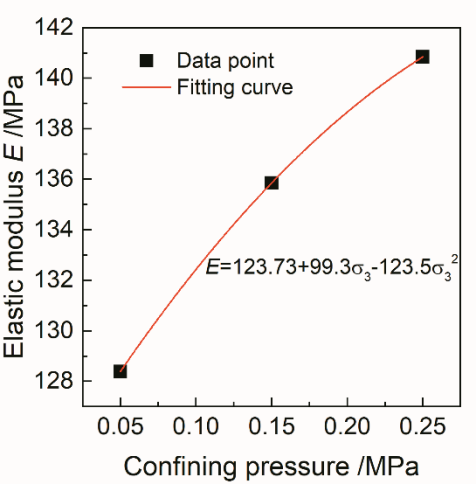

Figure3.*Fitting curve of the relationship between elastic modulus and confining pressure*

4.2 Parameter determination of damage model

According to the data in Figure. 1, the shape parameter m and scale parameter a of the stress damage model are solved by the above two methods. The final settlement results are shown in Table 3 and Table 4. Among them, Table 3 is the full fitting formula of formula (12), (24), (25), (26) and (27) in method 1; Table 4 is the semi theoretical semi fitting formula of formula (51), (54) and (55) in method 2.

Table 3.*Summary of Solution of Shape Parameter m and Scale Parameter a (Method 1)*

Temperature/℃	-0.3		-1.0		-2.0	
Confining pressure /MPa	*m*	*a*	*m*	*a*	*m*	*a*
0.05	1.3680	12.8596	1.3090	14.4286	1.4080	16.4050
0.15	1.3030	13.5591	1.2170	14.9914	1.2840	16.9624
0.25	1.2650	14.3200	1.1850	15.4883	1.2530	17.3285

Table 4.*Summary of Solution of Shape Parameter m and Scale Parameter a (Method 2)*

Temperature/℃	-0.3		-1.0		-2.0	
Confining pressure /MPa	*m*	*a*	*m*	*a*	*m*	*a*
0.05	1.3452	12.9657	1.3501	14.4209	1.3412	16.5967
0.15	1.3206	13.5783	1.2086	15.1146	1.2834	17.0735
0.25	1.3046	14.2468	1.1698	15.6325	1.2692	17.5389

In order to obtain the stress-strain curve under the condition of nonparametric experimental confining pressure, polynomial fitting is used to fit the relationship between the shape parameter m and scale parameter a with the confining pressure.

Fit the parameter value when the experimental temperature is -2℃, and the fitting curve is as shown in Figure. 4.

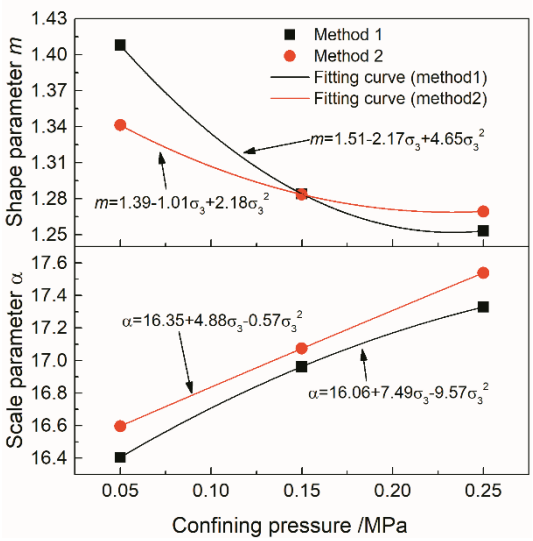

Figure4.*Fitting curve of shape parameter m and scale parameter a to the change of confining pressure*

The final fitting polynomial is shown in the following formula, where equation (60) is the parameter fitting equation obtained by method 1, and equation (61) is the parameter fitting equation obtained by method 2.

$$\begin{cases} m = 1.51 - 2.17\sigma_3 + 4.65\sigma_3^2 \\ a = 16.06 + 7.49\sigma_3 - 9.57\sigma_3^2 \end{cases} \tag{60}$$

$$\begin{cases} m = 1.39 - 1.01\sigma_3 + 2.18\sigma_3^2 \\ a = 16.35 + 4.88\sigma_3 - 0.57\sigma_3^2 \end{cases} \tag{61}$$

4.3 Verification of experimental results

According to the above constant temperature to determine the confining pressure triaxial compression test results and the parameters obtained from calculation and analysis, the model is verified. First of all, the non-destructive state of the temperature damage calculation is taken as -

2.0℃, and the stress-strain curves at -0.3℃ and -1.0℃ are reconstructed with the data parameters, and compared with the experimental curves.

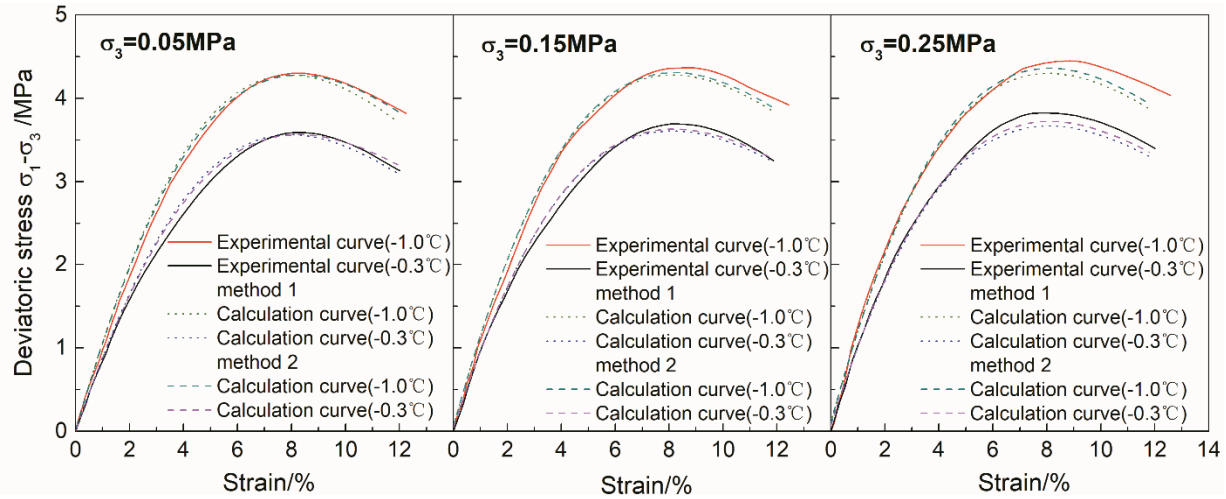

Figure5.*Comparison of the calculated values of -0.3℃ and -1.0℃ damage models when -2.0℃ is the non-destructive temperature*

It can be seen from Figure. 5 that the overall simulation results of the model are good, among which the model simulation results are the most accurate when the confining pressure is 0.05MPa, and there is a certain deviation when the bias stress simulation is 0.25MPa. By comparing the simulation accuracy of the three groups of confining pressure curves to the original experimental curves, it can be found that with the increase of confining pressure, the deviation degree of the calculated curves from the experimental curves increases gradually. At the same time of confining pressure, the model is more accurate for the experimental simulation results with higher temperature.

The influence of the two methods on the simulation results is compared. As can be easily seen from Figure. 5, the simulation results of the parameters obtained by method 2 are closer to the experimental curve than those obtained by method 1. When the confining pressure is small, the difference between the two methods is not big, but with the increase of confining pressure, the difference between the calculation curve of method 2 and the experimental curve is obviously smaller than that of method 1. The above verification process shows that the simulation results of the stress temperature coupled damage model have a high accuracy under the condition that the stress damage amount and the temperature damage amount corresponding to the target temperature are known.

Furthermore, through the temperature controlled triaxial compression experiment, the simulation prediction ability of the model to the actual stress-strain curve is verified when the model parameters are predicted according to the fitting polynomials in the preset stress and temperature range.

Three groups of experimental conditions were selected:① the confining pressure was 0.10MPa, and the experimental temperature was -0.3℃;②the confining pressure was 0.05MPa, and the experimental temperature was -1.3℃;③ the confining pressure was 0.10MPa, and the experimental temperature was -1.3℃.According to equations (58), (59) and (61), the parameters

required for the model calculation under the corresponding temperature and confining pressure are calculated, and the calculation results are shown in Table 5.

Table 5.*Calculation Results of Damage Model Parameters Fitting Polynomials*

Confining pressure /MPa	0.05				0.10			
Temperature/°C	E_T	E	m	a	E_T	E	m	a
-0.3	91.02	128.39	1.3450	16.5926	91.02	132.43	1.3108	16.8323
-1.3	115.77				115.77			

According to the parameters in Table 5, the final calculation curve is compared with the experimental curve as shown in Figure. 6.

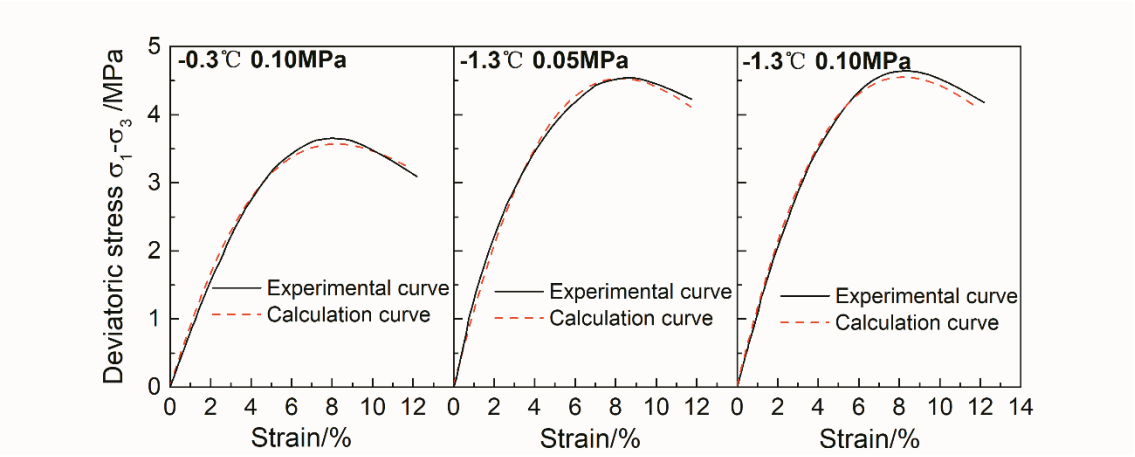

Figure6.*Comparison between experimental curve and calculation curve of temperature controlled triaxial compression test*

It can be seen from Figure. 6 that the calculation curve obtained by using the damage model parameters can accurately simulate the stress growth with strain in the stress growth stage, while in the stress peak prediction, the simulation results under the condition of small confining pressure are still better than those under the condition of large confining pressure.

In the three groups of verification experiments shown in Figure. 6, the first two groups of experimental verification calculation respectively used the fitting values of the elastic modulus E corresponding to 0.10MPa at -2.0°C, the double parameters of Weibull distribution and the elastic modulus E_T representing temperature damage, while the third group used the fitting calculation formula for all the above four parameters. Compared with the simulation results, it is not difficult to find that there is a certain difference between the fitting value and the actual value, and the more the difference is introduced, the greater the impact on the results will be. Therefore, in the process of practical application, we should try to ensure that the experimental conditions of parameters are close to the actual working conditions, so as to improve the simulation accuracy.

5 Model discussion

As two important factors affecting the mechanical properties of frozen soil, confining pressure and temperature are a problem that must be faced in the practical application of damage model(Nassr et al., 2018; Xu, Xiangtian et al., 2019). In most cases, the experimental conditions

of parameters can not fully correspond to the actual conditions, so the fitting prediction of model parameters can not be avoided. It is easy to see from Table 2 and Table 4 that the elastic modulus E, shape parameter m and scale parameter a all change with the confining pressure and temperature. The stress-strain curve of frozen soil is predicted only by stress damage without considering the coupling damage of stress and temperature. Therefore, the parameter values corresponding to different confining pressures and temperatures are expressed by binary polynomials, and the parameters are predicted according to the polynomials.

The fitting polynomials are as follows.

$$E = 79.76 + 27.63|T| + 76.24\sigma_3 - 2.63|T|^2 - 101.67\sigma_3^{\,2} + 6.87|T|\cdot\sigma_3 \tag{62}$$

$$a = 11.8974 + 2.2915|T| + 7.5042\sigma_3 - 0.0416|T|^2 - 2.1883\sigma_3^{\,2} - 1.0208|T|\cdot\sigma_3 \tag{63}$$

$$m = 1.4941 - 0.2381|T| - 1.2088\sigma_3 + 0.1002|T|^2 + 2.5817\sigma_3^{\,2} - 0.0489|T|\cdot\sigma_3 \tag{64}$$

At the same time, it can be seen from Table 2 that the friction angle and Poisson's ratio also change with the change of temperature, and the polynomial fitting method is still used for prediction.

$$\varphi = 25.24 - 13.49|T| + 4.10|T|^2 \tag{65}$$

$$v = 0.2687 - 0.0231|T| + 0.0057|T|^2 \tag{66}$$

According to formula (58) - (66), calculate the experimental parameter data of temperature controlled triaxial compression described in the previous section, and compare the calculation results of stress temperature coupled damage model, as shown in Figure. 7.

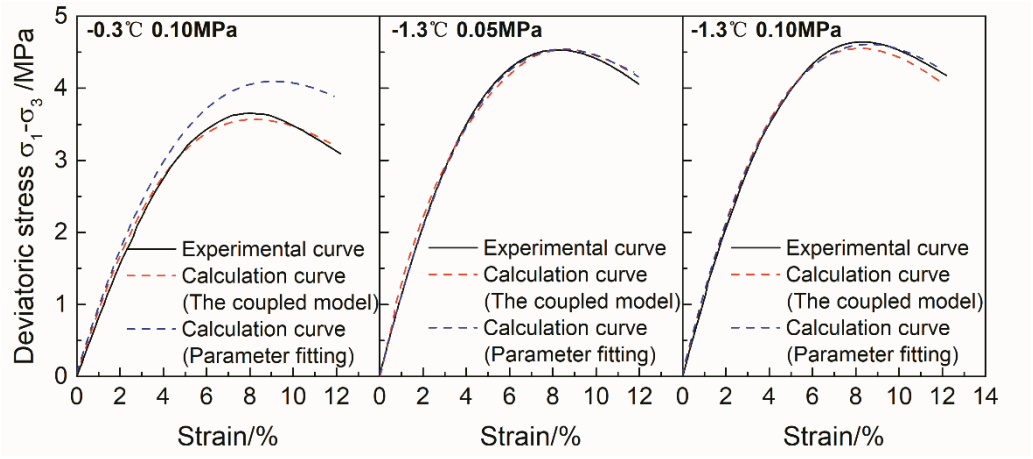

Figure7.*Comparison of results of stress-temperature coupled model and conventional parameter fitting*

It can be seen from Figure. 7 that the simulation results of the latter two groups of experiments are more accurate only by parameter fitting. When the temperature is -1.3℃ and the confining pressure is 0.10MPa, the simulation results are even better than the stress-temperature coupled damage model to some extent. However, the simulation results of the first group of experiments gradually deviate from the actual stress-strain curve in the stress growth stage, and the deviation of the final simulation results is too large.

Now the error sources of the above simulation methods are analyzed. Based on the calculation parameters of the damage model under the experimental temperature of -0.3℃ and the experimental confining pressure of 0.05MPa, the influence of 10% increase or decrease of each parameter on the calculation curve is compared. The final result is shown in Figure. 8.

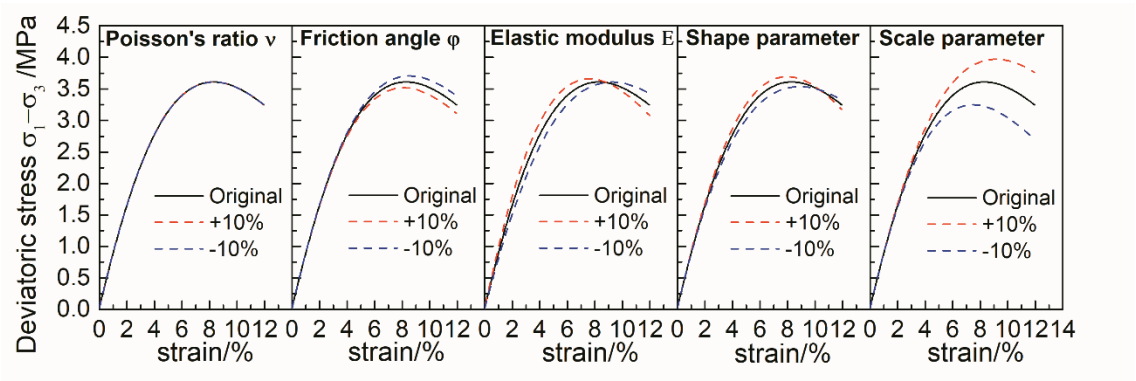

Figure8.*Comparison of the influence of 10% increase and 10% decrease of each parameter of the model on the calculation curve*

When each parameter increases or decreases by 10% on the original datum parameter, the Poisson's ratio ν error has negligible effect on the final calculation curve compared with the original calculation curve. The influence of the error of friction angle φ and scale parameter a on the calculation results is mainly reflected in the peak value. With the increase of friction angle φ, the peak strain decreases and the peak deviator stress decreases. On the contrary, with the increase of the scale parameter a, the peak deviator stress and strain increase simultaneously. The friction angle φ increases by 10%, the peak strain decreases by 2.41% and the peak deviator stress decreases by 2.55%. The friction angle φ decreases by 10%, the peak strain increases by 2.41% and the peak deviator stress increases by 2.71%. When the scale parameter a increases or decreases by 10%, the peak strain increases or decreases by 10.25% compared with the reference value, and the peak deviator stress increases or decreases by 10.01%. It can be seen that the model results are more sensitive to the changes of scale parameters a.

The elastic modulus E and the shape parameter m have an effect on the stress growth, the peak value of stress and the stress decline stage of the calculation curve, and their overall change trends are the same. In the stress growth stage, the larger the parameter value is, the faster the stress growth is, and the stress growth caused by the change of elastic modulus E is more significant than that caused by the change of shape parameter m. In the part of peak stress, with the increase of parameter value, the peak strain decreases and the peak deviator stress increases; the change of elastic modulus E has more significant effect on the peak strain, while the shape parameter m has more obvious effect on the peak deviator stress. In the stress decreasing stage, the smaller the parameter value is, the slower the decreasing speed is, and the calculation curve is more sensitive to the change of elastic modulus E in this stage.

From the above diagram and analysis, it can be seen that the other four parameters except Poisson's ratio ν have a certain impact on the reconstruction curve. Under the condition of the same amplitude change, the influence of scale parameter a is the most obvious. Further comparative analysis: when multiple parameters change at the same time, the difference between

the reconstruction curve and the reference curve will not be discussed because Poisson's ratio ν has little influence on the reconstruction curve. The final result is shown in Figure 9.

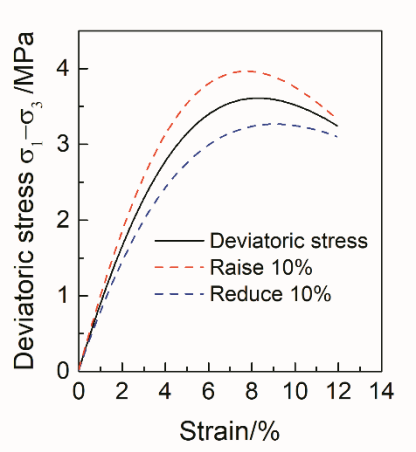

Figure9.*Comparison of the influence of 10% increase or decrease of multi parameters of the model on the calculation curve*

It is not difficult to find out from Figure. 9 that when multiple parameters change at the same time, the influence of each parameter will have a composite superposition effect, and the three stages of reconstruction stress-strain curve deviate greatly from the original datum curve. The variation of peak deviator stress is mainly due to the error of scale parameter a, and the deviation of stress growth stage is mainly due to the change of elastic modulus E and shape parameter m. The more fitting parameters are, the greater the influence of model parameter error on reconstruction curve accuracy is.

It can be seen from Table 4 that when the change of confining pressure and temperature is small, the change range of shape parameter m and scale parameter a is not large, but the final result is very sensitive to the change of these two parameters[18]. When the binary polynomial fitting is used, the error of parameter simulation value will be further enlarged compared with that of single variable polynomial fitting. When the two parameters have errors at the same time, the uncertainty of the model will rise sharply, resulting in the reliability of the final result.

To sum up, it is necessary to predict the elastic modulus E, shape parameter m, scale parameter a, Poisson's ratio ν and friction angle φ under a certain target temperature and confining pressure state (non parametric experimental state) when the stress-strain curve of warm frozen soil is simulated simply by using the stress damage model. Among them, the elastic modulus E, shape parameter m andscale parameter a are affected by temperature and confining pressure changes at the same time, so binary function is needed to fit them. When using the coupled stress temperature damage model, only the shape parameter m, scale parameter a, Poisson's ratio ν and the elastic modulus E at the target temperature are estimated. And different from the single stress damage model, the parameters needed in the stress-temperature coupled damage model can be fitted by only one element polynomial, which greatly reduces the uncertainty of parameter prediction.

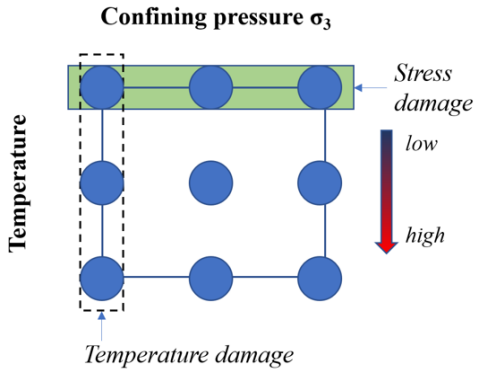

Figure10.*Schematic diagram of experimental conditions of model parameters*

Further compare the minimum experimental amount of the two parameter experiments. As shown in Figure. 10, in a certain temperature and confining pressure condition area, in order to predict any point, a single stress damage model needs at least 9 groups of experimental data to fit the parameters. However, if the stress-temperature coupled damage model is used, the temperature damage factor can be determined only by the experimental data of three groups of different confining pressures under the lowest temperature in the condition area, and the experimental data of three groups of different temperatures under any one of the three confining pressures, and the temperature damage factor can be determined, and the total minimum required is five groups of experimental data.

It can be seen that the stress-temperature coupled damage model is superior to the single stress-strain damage model in terms of the prediction accuracy of the stress-strain curve corresponding to the model and the experimental parameters.

6 Conclusion

Based on Hooke's law and strain equivalent theory of damage mechanics, the damage model of warm frozen soil structure under the coupling action of three-dimensional stress and temperature (stress-temperature coupled damage model) is established by using Weibull distribution to describe the damage of warm frozen soil element. Through theoretical analysis, mathematical derivation and experimental verification, the following conclusions are obtained:

(1) The composite damage theory is introduced into the stress-temperature coupled damage model of warm frozen soil. Based on Mohr-Coulomb criterion, the nominal stress is used to represent the stress damage of permafrost element, the initial elastic modulus is used to represent the temperature damage, and the composite damage factor is introduced to describe the coupling relationship between them, which makes the model more meaningful in theory.

(2) There are two general methods to solve the shape parameter m and scale parameter a of the stress temperature coupled damage model. Experimental results show that: for strain softening materials, when the confining pressure level is low, the difference between the two methods is small. However, under high confining pressure, the reconstruction curve obtained by the semi theoretical semi fitting method based on the characteristic points of the stress-strain curve is closer to the experimental curve.

(3) The results of triaxial compression experiments with constant temperature confining pressure show that the stress-temperature coupled damage model has good simulation and prediction ability. In the stage of stress development, the overall prediction accuracy of the model is high; in the stage of stress peak, the prediction accuracy of the model decreases slightly with the increase of confining pressure; in the same confining pressure, the prediction accuracy of the model increases with the increase of the temperature of frozen soil.

(4) Compared with the single stress damage model, the stress-temperature coupled damage model needs less model parameters, and only needs the one-dimensional function fitting to complete the prediction. It can effectively reduce the influence of the system error caused by the parameter estimation on the final results, effectively reduce the workload of the parameter experiment, and improve the stability of the model.

Acknowledgments

Data used in this study is new data for the first time created for this research. We thank for National Natural Science Foundation of China (41641024) for providing financial support.

References

Cao, W., & Zhang, S. (2005). Study on the statistical analysis of rock damage based on Mohr-Coulomb criterion. Journal of Hunan University, 32(1), 43-47.

Dumais, S., & Konrad, J. M. (2017). One-dimensional large-strain thaw consolidation using nonlinear effective stress–void ratio–hydraulic conductivity relationships. Canadian Geotechnical Journal, 55(3), 414-426. doi:https://doi.org/10.1139/cgj-2017-0221

Esmaeili-Falak, M., Katebi, H., Javadi, A., & Rahimi, S. (2017). Experimental investigation of stress and strain characteristics of frozen sandy soils-A case study of Tabriz subway. Modares Civil Engineering journal, 17(5), 13-23.

Jia, H., Zi, F., Yang, G., Li, G., Shen, Y., Sun, Q., & Yang, P. (2019). Influence of Pore Water (Ice) Content on the Strength and Deformability of Frozen Argillaceous Siltstone. Rock Mechanics Rock Engineering, 1-8.

Jin, X., Yang, W., Meng, X., & Lei, L. (2019). Deduction and application of unfrozen water content in soil based on electrical double-layer theory. Rock and Soil Mechanics, 40(04), 1449-1456.

Lai, Y., Jin, L., & Chang, X. (2009). Yield criterion and elasto-plastic damage constitutive model for frozen sandy soil. International Journal of Plasticity, 25(6), 1177-1205.

Lai, Y., Li, S., Qi, J., Gao, Z., & Chang, X. (2008). Strength distributions of warm frozen clay and its stochastic damage constitutive model. Cold Regions Science Technology, 53(2), 200-215. doi:https://doi.org/10.1016/j.coldregions.2007.11.001

Lemaitre, J. (2012). A course on damage mechanics, Springer Science & Business Media.

Li, G. (2009). Some problems in researches on constitutive model of soil. Chinese Journal of Geotechnical Engineering, 10.

Li, S., Lai, Y., Zhang, M., & Zhang, S. (2007). Study on distribution laws of elastic modulus and strength of warm frozen soil. Chinese Journal of Rock Mechanics Engineering, 26, 4299-4305.

Li, S., Lai, Y., Zhang, S., & Liu, D. (2009). An improved statistical damage constitutive model for warm frozen clay based on Mohr–Coulomb criterion. Cold Regions Science and Technology, 57(2), 154-159. doi:https://doi.org/10.1016/j.coldregions.2009.02.010

Liu, S., & Zhang, J. (2012). Review on physic-mechanical properties of warm frozen soil. Journal of Glaciology Geocryology, 34(1), 120-129.

Liu, Z., & Yu, X. (2011). Coupled thermo-hydro-mechanical model for porous materials under frost action: theory and implementation. Acta Geotechnica, 6(2), 51-65. doi:https://xs.scihub.ltd/https://doi.org/10.1007/s11440-011-0135-6

Ma, W., Wu, Z., Zhang, L., & Chang, X. (1999). Analyses of process on the strength decrease in frozen soils under high confining pressures. Cold Regions Science Technology, 29(1), 1-7. doi:https://doi.org/10.1016/S0165-232X(98)00020-2

Na, S., & Sun, W. (2017). Computational thermo-hydro-mechanics for multiphase freezing and thawing porous media in the finite deformation range. Computer Methods in Applied Mechanics Engineering, 318, 667-700. doi:https://doi.org/10.1016/j.cma.2017.01.028

Nassr, A., Esmaeili-Falak, M., Katebi, H., &Javadi, A. (2018). A new approach to modeling the behavior of frozen soils. Engineering geology, 246, 82-90. doi:https://doi.org/10.1016/j.enggeo.2018.09.018

Ning, J., & Zhu, Z. (2007). Constitutive model of frozen soil with damage and numerical simulation of the coupled peoblem. Chinese Joumal of Theoretical Applied Mechanics, 1.

Qi, J., & MA, W. (2010). State-of-art of research on mechanical properties of frozen soils. Rock Soil Mechanics, 31(1), 133-143.

Song, B., Liu, E., & Zhang, D. (2019). Experimental study on the mechanical properties of warm frozen silt soils. Journal of Glaciology and Geocryology, 41(03), 595-605.

Wei, Z., Jin, H., Zhang, J., Yu, S., Han, X., Ji, Y., He, R., & Chang, X. (2011). Prediction of permafrost changes in Northeastern China under a changing climate. Science China Earth Sciences, 54(6), 924-935.

Xu, W., & Wei, L. (2002). Study on statistical damage constitutive model of rock. Chinese Journal of Rock Mechanics Engineering, 21(6), 787-791.

Xu, X., Li, Q., Lai, Y., Pang, W., & Zhang, R. (2019). Effect of moisture content on mechanical and damage behavior of frozen loess under triaxial condition along with different confining pressures. Cold Regions Science Technology, 157, 110-118. doi:https://doi.org/10.1016/j.coldregions.2018.10.004

Xu, X., Wang, J., & Zhang, L. (2001). Frozen soil physics. Beijing, Beijing Science Technology Press, .

Xu, X., Wang, Y., Bai, R., Zhang, H., & Hu, K. (2016). Effects of sodium sulfate content on mechanical behavior of frozen silty sand considering concentration of saline solution. Results in physics, 6, 1000-1007. doi:https://doi.org/10.1016/j.rinp.2016.11.040

Yan, C., Wang, T., Jia, H., Xu, W., & Zi, F. (2019). Influence of the unfrozen water content on the shear strength of unsaturated silt during freezing and thawing. Chinese Journal of Rock Mechanics and Engineering, 38(06), 1252-1260.

Yu, S., Deng, H., & Zhang, Y. (2018). The constitutive relationship of rock damage considering the effect of temperature and confining pressure. Journal of Railway Science Engineering, 15, 1-9.

Zhang, D., Liu, E., Liu, X., Zhang, G., Yin, X., & Song, B. (2018). A damage constitutive model for frozen sandy soils based on modified Mohr-Coulomb yield criterion. Chinese Journal of Rock Mechanics Engineering, 37(4), 978-986.

Zhang, H., & Yang, G. (2010). Research on damage model of rock under coupling action of freeze-thaw and load. Chinese Journal of Rock Mechanics Engineering, 29(3), 471-476.

Zhang, M., Pei, W., Li, S., Lu, J., &Jin, L. (2017). Experimental and numerical analyses of the thermo-mechanical stability of an embankment with shady and sunny slopes in a permafrost region. Applied Thermal Engineering, 127, 1478-1487. doi:https://doi.org/10.1016/j.applthermaleng.2017.08.074

Zhang, Y., & Michalowski, R. L. (2015). Thermal-hydro-mechanical analysis of frost heave and thaw settlement. Journal of geotechnical geoenvironmental engineering, 141(7), 04015027. doi:https://doi.org/10.1061/(ASCE)GT.1943-5606.0001305

Zhou, Y., Guo, D., Qiu, G., Cheng, G., & Li, S. (2000). Geocryology in China. Beijing, Chinese Academy of Sciences.